Blocking Harmful Blue Light while Preserving Image Color Appearance

Kuang-Tsu Shih, Jen-Shuo Liu, Frank Shyu, Su-Ling Yeh, and Homer H. Chen*
National Taiwan University

(a) Original image (b) Distorted image (c) Our result (d) Emisson spectrum at point A (e) Emisson spectrum at point B

Figure. 1: *Applying a blue light blocker to a display panel introduces image color distortion. Specifically, the hue of the image is biased towards red and yellow, as shown in (b). The proposed approach blocks the harmful blue light while preserving the image color appearance, as shown in (c). The emission spectra of the display at points A and B are shown in (d) and (e), respectively. The color of B is identical to A, but the spectrum of B has nearly zero power in the sensitive band of the ipRGC, a newly discovered light sensitive cell that suppresses the secretion of melatonin.*

Abstract

Recent study in vision science has shown that blue light in a certain frequency band affects human circadian rhythm and impairs our health. Although applying a light blocker to an image display can block the harmful blue light, it inevitably makes an image look like an aged photo. In this paper, we show that it is possible to reduce harmful blue light while preserving the blue appearance of an image. Moreover, we optimize the spectral transmittance profile of blue light blocker based on psychophysical data and develop a color compensation algorithm to minimize color distortion. A prototype using notch filters is built as a proof of concept.

Keywords: computational display, blue light, vision science

Concepts: • Human-centered computing ~ Displays and imagers; Computing methodologies ~ Image processing; Applied computing ~ Consumer health; *Applied computing ~Psychology;*

1 Introduction

We are exposed to electronic displays day and night nowadays, but this may not be good for our health. Scientists have found numerous evidences showing that exposing to blue light emitted from the display during nighttime greatly affects our circadian clock and can do serious harm to our health. For example, it has been shown that using electronic displays at night prolongs the time needed to fall asleep [Chang et. al 2015] and that exposing to blue light at night may be related to the causation of breast cancer [Stevens et al. 2009] and obesity [Stevens et al. 2007]. Many other studies also pointed to the same conclusion that blue light has adverse health effects [Harvard 2012].

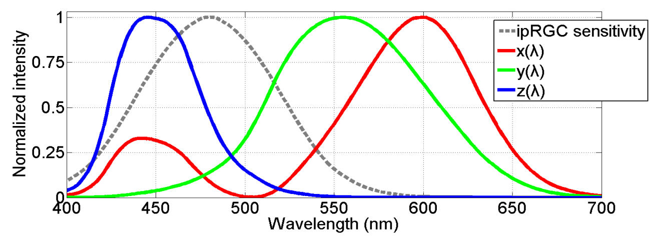

Figure. 2: *The spectral sensitivity profile of ipRGC and the three CIE 1931 color matching functions.*

One may reduce the blue light by placing a frequency-selective light blocker in front of the display [Lely et al. 2014] or using an app to suppress the intensity of blue pixels. However, as illustrated in Fig. 1(b), a blue light blocker can easily destroy color fidelity, because the elimination of blue light causes the hue of the image to bias towards red and yellow.

Therefore, we ask two fundamental questions:

- Is it possible at all to remove the harmful blue light without affecting color fidelity?
- If it is possible, what is the optimal way?

In this paper, we address these questions and propose an effective solution. Our approach is motivated by the research findings about the cause of blue light related disorders. Vision scientists believe that such disorders are closely related to a newly discovered light sensitive cell called "intrinsically photosensitive retinal ganglion cell" (ipRGC) on our retina [Berson et al. 2002]. Unlike ordinary ganglion cells, ipRGC has its own photopigment that can be triggered by light, similar to the cone and rod [Berson et al. 2002; Zaidi et. al 2007]. It has been shown that our circadian clock has to do with the ipRGC response, which can impair our health if it is too strong [Berson et al. 2003].

To reduce harmful blue light without degrading the blue image appearance, we create a metameric match of the input light spectrum such that the compensated spectrum results in a color sensation nearly identical to the original spectrum but induces minimal ipRGC response. Fig. 2 shows the spectral sensitivity profile of the ipRGC obtained by vision scientists [Dacey et al. 2005; Gamlin et al. 2007] and the three CIE 1931 color matching

*On leave at UCLA

SA '16 Technical Papers, December 05-08, 2016, Macao
© 2016 ACM. ISBN 978-1-4503-4514-9/16/12$15.00
DOI: http://dx.doi.org/10.1145/2980179.2982418

ACM Reference Format
Shih, K., Liu, J., Shyu, F., Yeh, S., Chen, H. 2016. Blocking Harmful Blue Light while Preserving Image Color Appearance. ACM Trans. Graph. 35, 6, Article 175 (November 2016), 10 pages.
DOI = 10.1145/2980179.2982418 http://doi.acm.org/10.1145/2980179.2982418.

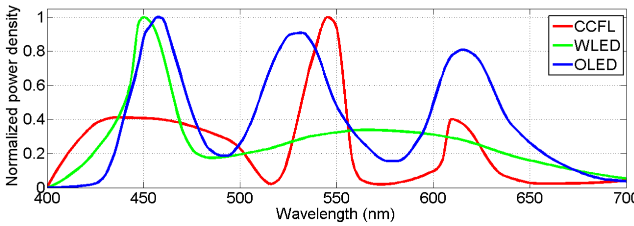

Figure. 3: *The emission spectra of a cold cathode fluorescent lamp (CCFL), a white light-emitting diode (WLED), and an organic light-emitting diode (OLED).*

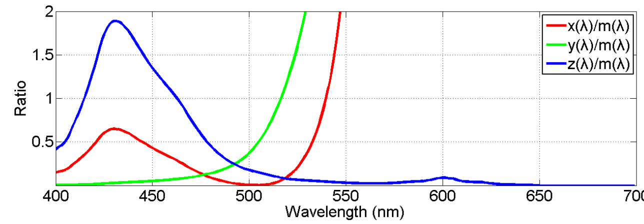

Figure. 4: *The ratio of the CIE 1931 color matching functions to the spectral sensitivity profile of ipRGC.*

functions. We can see that the peak of the ipRGC sensitivity profile deviates from those of the three matching functions, suggesting that it is possible to preserve the color sensation while reducing the ipRGC response.

The importance of this work cannot be overstated because most existing displays that we use every day contain a light source that emits blue light. Fig. 3 shows the emission spectra of a cold cathode fluorescent lamp (CCFL), a white light-emitting diode (WLED), and an organic light-emitting diode (OLED). We can see that the spectral power density of these light sources is non-zero near 482 nm, which is the most sensitive frequency of ipRGC. Since these light sources are widely employed in desktop monitors, televisions, smart phones, and tablet computers that are indispensable in our lives, a solution that minimizes the harm without degrading user experience is valuable.

Our main contributions are summarized as follows:

- We show that it is possible to preserve the blue image appearance and reduce the harmful blue light.
- Based on the spectral sensitivity profile of ipRGC, we provide a theoretical foundation for the design of a frequency-selective light blocker that maximizes the display gamut and blocks the blue light in the most harmful frequency band.
- Our color compensation method compensates for the color distortion caused by a blue light blocker.
- We realize a proof-of-concept prototype and show that it indeed reduces the harmful blue light without introducing color distortion.

2 Background

The blue light sensitive cell ipRGC has profound impact on our health. To help understand what "harmful blue light" means, we provide a brief review of the spectral and psychophysical properties of ipRGC. To help understand why it is possible to preserve the color appearance of an image in the absence of a blue frequency band in the light spectrum, we discuss the basic theory about color perception; that is, how a light spectrum is perceived by our brain. Specifically, we discuss the condition under which two distinct light spectra result in identical color sensation. The information discussed in this section serves as the basis of our approach.

ipRGC Not all blue lights are equally harmful. Recent research in vision science [Berson et al. 2002] has revealed that there are actually two kinds of blue light sensitive cells in our eyes, namely, the ipRGC and the S-cone that is responsible for our perception of the color "blue." Interestingly, although ipRGC and S-cone are both sensitive to blue light, their most sensitive frequencies differ. Specifically, the peak of the spectral sensitivity of ipRGC is approximately at 482nm (Fig. 2) [Dacey et al. 2005; Gamlin et al. 2007], while that of S-cone is at around 440nm (or lower, depending on its adaptation state). This gap implies that, although both are perceived as "blue," the light with a frequency closer to 440nm actually induces less ipRGC response compared to the light with a frequency closer to 482nm. In this paper, we define the "harmful blue light" as the light with frequency close to the peak frequency of ipRGC. Although light in some other frequency bands may also be harmful to our health (e.g. macular degeneration, cataract, etc.), we only focus on the frequency band of ipRGC response in this paper. It should be clear that the proposed approach can be applied to deal with other frequency bands.

Why does ipRGC response impair our health? It is all about the melatonin—a hormone in our body. Melatonin is also known as the "hormone of darkness" and is usually produced at night by the pineal gland. It improves our sleep quality. Scientists believe that ipRGC response suppresses the secretion of melatonin. Therefore, they suggest that we avoid exposing to the particular band of blue light that induces ipRGC response at nighttime. Further study show that exposure to blue light in the evening prolongs our circadian cycle and decreases our alertness in the next morning [Chang et al. 2015] and that inappropriate exposure to blue light is related to seasonal affective disorder [Roecklein et. al. 2009], breast cancer [Stevens et al. 2009], and obesity [Stevens et al. 2007].

Unlike the cone and rod [Wanat et al. 2014], the ipRGC barely adapts to the viewing condition [Wong et al. 2012]. It works just like a photon counter, meaning that its response is approximately proportional to the power of the input light. This property allows us to directly focus on the spectral power of the light and ignore the other factors (such as viewing condition) that determine the adaptation level of the eyes. In addition, ipRGC is distributed evenly throughout the retina [Galindo-Romeroa et al. 2013]. This property allows us to ignore the position of the image on retina when computing the ipRGC response.

Metamerism In colorimetry, metamerism is a perceived matching of colors that appear to be identical but in fact have different spectral power distributions. Such colors are called metamers [Miyazaki et al. 2012]. This can be understood by noting that color is a subjective psychological phenomenon, and hence the perception of a color is dissociated from the physical spectrum of the color. In other words, color is a feature of the visual perception of an observer, not a property of the light spectrum [Morovic 2008].

Mathematically speaking, the light spectrum is a function on $\mathbb{R}^1$. It has infinite degrees of freedom, because the spectral power of the light at any frequency (a real number) can have its own value. However, there are only three types of cone cells on human retina. Consequently, there must exist multiple spectra that induce identical cone response and hence identical color sensation. If two different spectra result in identical color sensation, they are referred to as a "metameric match" of each other.

According to the color matching experiment performed in 1931 [Smith et al. 1931], two spectra $I_1(\lambda)$ and $I_2(\lambda)$ are a pair of metameric matches if

$$\begin{cases} \int I_1(\lambda)\bar{x}(\lambda)d\lambda = \int I_2(\lambda)\bar{x}(\lambda)d\lambda \\ \int I_1(\lambda)\bar{y}(\lambda)d\lambda = \int I_2(\lambda)\bar{y}(\lambda)d\lambda \\ \int I_1(\lambda)\bar{z}(\lambda)d\lambda = \int I_2(\lambda)\bar{z}(\lambda)d\lambda \end{cases}, \tag{1}$$

where $\bar{x}(\lambda)$, $\bar{y}(\lambda)$ and $\bar{z}(\lambda)$ are constant functions called the color matching functions and shown in Fig. 2.

3 Our Approach

This work aims at blocking the harmful blue light without changing the image color appearance. Although these two objectives seem contradictory to each other at the first glance, we show that they can be achieved at the same time.

Our main idea is to replace the spectrum of an image by a metameric match that induces the minimum ipRGC response. This is possible because the correlation between the spectral sensitivity profile of ipRGC and the XYZ color matching functions is adequately low (see Fig. 2). Although the spectral sensitivity profile of ipRGC is close to $\bar{z}(\lambda)$, its peak deviates from that of $\bar{z}(\lambda)$. We plot in Fig. 4 the ratio of $\bar{x}(\lambda)$, $\bar{y}(\lambda)$ and $\bar{z}(\lambda)$ to the spectral sensitivity profile $m(\lambda)$ of ipRGC. It can be seen that the ratio $\bar{z}(\lambda)/m(\lambda)$ has a peak value larger than 1 near 430nm. This observation suggests that, if the spectral power of the metameric match is more concentrated at 430nm, the ipRGC response can be better reduced.

Despite the above observation, directly manipulating the emission spectrum of a display is usually not possible because the spectra of the primaries in most existing displays are fixed. To make our solution practical, we combine a passive frequency-selective light blocker together with a color compensation algorithm.

4 Blue Light Blocker

In this section, we describe the design of the blue light blocker. We first derive the representation of display gamut volume and the expected ipRGC response as functions of the blocker's spectral transmittance and then formulate the design of the blocker as an optimization problem.

Display gamut volume Given the linearized RGB value $(R, G, B)\in[0, 1]\times[0, 1]\times[0, 1]$ ($\times$ denotes Cartesian product) of a pixel, the emission spectrum $d(\lambda)$ at the pixel can be described by

$$d(\lambda) = Rr(\lambda) + Gg(\lambda) + Bb(\lambda), \tag{2}$$

where $r(\lambda)$, $g(\lambda)$, and $b(\lambda)$ are the spectra of the three corresponding display primaries [Shih et al. 2016; Lindbloom 1989]. Let $F(\lambda)$ denote the spectral transmittance profile of the blue light blocker. Then, the emission spectrum after applying the light blocker is $F(\lambda)d(\lambda)$.

Next, we derive the relation between the RGB value and the resulting XYZ value. For the ease of expression, we define the inner product of functions by

$$\langle f_1, f_2 \rangle = \int_{400nm}^{700nm} f_1(\lambda) f_2(\lambda) d\lambda. \tag{3}$$

With this notation, the resulting XYZ value is derived as follows (we omit λ to keep the equations neat):

$$\begin{aligned} \begin{pmatrix} X \\ Y \\ Z \end{pmatrix} &= \begin{pmatrix} \langle Fd, \bar{x} \rangle \\ \langle Fd, \bar{y} \rangle \\ \langle Fd, \bar{z} \rangle \end{pmatrix} = \begin{pmatrix} \langle F(Rr+Gg+Bb), \bar{x} \rangle \\ \langle F(Rr+Gg+Bb), \bar{y} \rangle \\ \langle F(Rr+Gg+Bb), \bar{z} \rangle \end{pmatrix} \\ &= \begin{pmatrix} \langle Fr, \bar{x} \rangle & \langle Fg, \bar{x} \rangle & \langle Fb, \bar{x} \rangle \\ \langle Fr, \bar{y} \rangle & \langle Fg, \bar{y} \rangle & \langle Fb, \bar{y} \rangle \\ \langle Fr, \bar{z} \rangle & \langle Fg, \bar{z} \rangle & \langle Fb, \bar{z} \rangle \end{pmatrix} \begin{pmatrix} R \\ G \\ B \end{pmatrix} \equiv \mathbf{H}_F \begin{pmatrix} R \\ G \\ B \end{pmatrix}, \end{aligned} \tag{4}$$

where $\bar{x}(\lambda)$, $\bar{y}(\lambda)$, and $\bar{z}(\lambda)$ represent the CIE 1931 color matching functions, and $\mathbf{H}_F$ denotes the transfer matrix from the linearized RGB domain to the XYZ domain. The subscript F is added to specify that the transfer matrix is determined by the spectral transmittance profile $F(\lambda)$ of the light blocker.

Having derived the relation between the XYZ value and the RGB value, we are now ready to derive the display gamut volume. By definition, the display gamut D is the set of all displayable XYZ values. That is,

$$D = \{(X, Y, Z) \mid 0 \le R, G, B \le 1\} \tag{5}$$

Considering (4) and (5) together, we obtain the volume of D in the XYZ space,

$$\|D\| = |\det \mathbf{H}_F|. \tag{6}$$

Expected ipRGC response Consider again the spectral sensitivity profile $m(\lambda)$ of ipRGC. The ipRGC response I induced by the spectrum $F(\lambda)d(\lambda)$ can be expressed by

$$\begin{aligned} I &= \langle Fd, m \rangle = \langle F(Rr+Gg+Bb), m \rangle \\ &= \left(\langle Fr, m \rangle \ \ \langle Fg, m \rangle \ \ \langle Fb, m \rangle \right) \left(R \ \ G \ \ B \right)^{\mathrm{T}} \\ &\equiv \mathbf{v}_F \left(R \ \ G \ \ B \right)^{\mathrm{T}}. \end{aligned} \tag{7}$$

Here we take the gray-world assumption that the expected value of R, G, and B are equal. Then, the expected ipRGC response is

$$\mathrm{E}[I] = \mathrm{E}[\mathbf{v}_F \left(R \ \ G \ \ B \right)^{\mathrm{T}}] = \mathbf{v}_F \mathrm{E}[\left(R \ \ G \ \ B \right)^{\mathrm{T}}] \propto \|\mathbf{v}_F\|_1. \tag{8}$$

Therefore, to lower the ipRGC response, it is desirable that the norm of $\mathbf{v}_F$ is as small as possible.

Optimizing the objective function Considering (6) and (8) together, we formulate the design of blue light blocker as a constrained optimization problem,

$$\begin{aligned} &\arg\min_{F(\lambda)} \left\{ -\left(\det \mathbf{H}_F\right)^2 + w_I \left(\|\mathbf{v}_F\|_2 \right)^6 \right\}, \\ &\text{subject to } 0 \le F(\lambda) \le 1, \ \forall \lambda \in [400\text{nm}, 700\text{nm}], \end{aligned} \tag{9}$$

where w_I is the weight assigned to the ipRGC response term. Note that we replace the L1-norm in (8) with an L2-norm to simplify the computation. Also note that we add the sixth power of the ipRGC response to the cost function to balance the first term, which is the square of the volume of a three-dimensional gamut. We solve (9) iteratively using the gradient descent method and handle the constraints by projecting the solution onto the boundary of the feasible region in each iteration.

5 Color Compensation

We describe the color compensation algorithm in detail in this section. The main concept behind the algorithm is as follows: If a

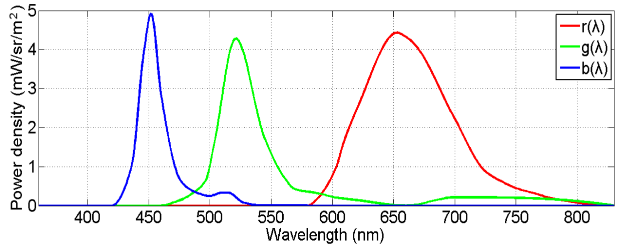

Figure. 5: *The emission spectra of the three primaries of the ASUS PA246Q liquid crystal display adopted in our experiment.*

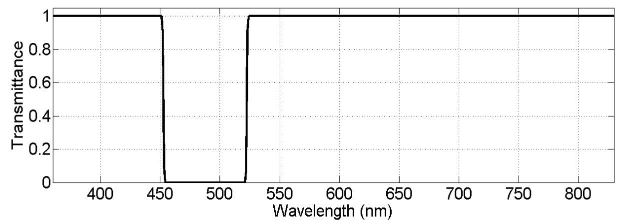

Figure. 6: *The resulting spectral transmittance profile of the optimized blue light blocker.*

pixel falls within the display gamut, its XYZ value is preserved; otherwise, we preserve its chroma and hue while compressing its lightness.

Let (R_o, G_o, B_o) denote the RGB value of an arbitrary pixel in the input image. To recover the color of the original image, it is required that the compensated RGB value (R_c, G_c, B_c), when shown on the display with a light blocker, result in an XYZ value identical to the original pixel. That is, we want (R_c, G_c, B_c) to be as close as possible to

$$\mathbf{H}_F^{-1}\mathbf{H}\begin{bmatrix} R_o & G_o & B_o \end{bmatrix}^{\mathrm{T}}, \tag{10}$$

where $\mathbf{H}$ represents the transfer matrix from the RGB space to the XYZ space of the display without a light blocker,

$$\mathbf{H} = \begin{pmatrix} \langle r,\bar{x}\rangle & \langle g,\bar{x}\rangle & \langle b,\bar{x}\rangle \\ \langle r,\bar{y}\rangle & \langle g,\bar{y}\rangle & \langle b,\bar{y}\rangle \\ \langle r,\bar{z}\rangle & \langle g,\bar{z}\rangle & \langle b,\bar{z}\rangle \end{pmatrix}. \tag{11}$$

However, the resulting RGB value obtained through (10) may not be in the range [0, 1] for some pixels, indicating that a perfect XYZ match is not possible due to the limited display gamut size.

To deal with such out-of-gamut pixels, we compute their in-gamut match (R_c, G_c, B_c) with identical hue and chroma but a compressed lightness. Specifically, we adopt the CIE $L^*C^*h^*$ color space to represent the perceptual attributes of lightness, chroma, and hue for its uniformity [Fairchild, 2005; Shapira et al. 2012]. Let $\Lambda(\cdot)$ denote the transformation from the XYZ space to the $L^*C^*h^*$ space. The LCh value (L_o, C_o, h_o) of the original image is then obtained by

$$\begin{bmatrix} L_o & C_o & h_o \end{bmatrix}^{\mathrm{T}} = \Lambda(\mathbf{H}\begin{bmatrix} R_o & G_o & B_o \end{bmatrix}^{\mathrm{T}}). \tag{12}$$

Next, we compute the lightness scaling ratio K and the compensated RGB value (R_c, G_c, B_c) by

$$\arg\max_K K,\ \text{subject to} \begin{cases} K \le 1 \\ 0 \le R_c, G_c, B_c \le 1 \end{cases}, \tag{13}$$

where

$$\begin{bmatrix} R_c & G_c & B_c \end{bmatrix}^{\mathrm{T}} = \mathbf{H}_F^{-1}\Lambda^{-1}(\begin{bmatrix} KL_o & C_o & h_o \end{bmatrix}^{\mathrm{T}}). \tag{14}$$

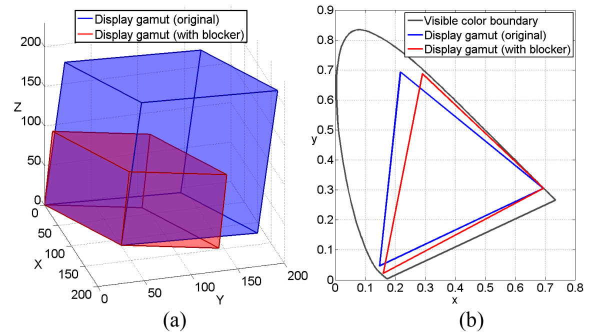

Figure. 7: *The display gamut before and after applying the optimized blue light blocker plotted in (a) the XYZ space and (b) the xy space.*

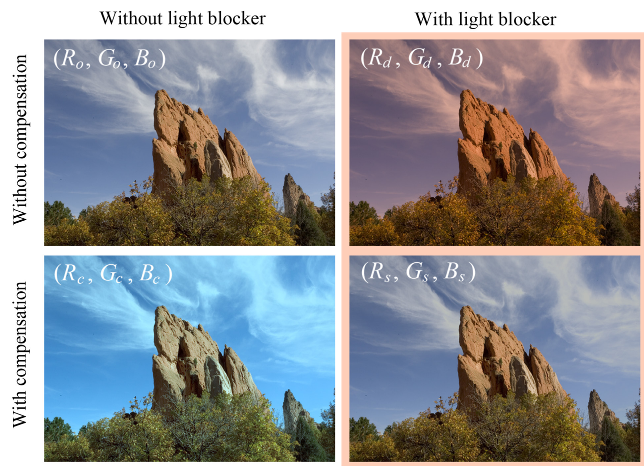

Figure. 8: *Illustration of* (R_o, G_o, B_o), (R_d, G_d, B_d), (R_c, G_c, B_c), *and* (R_s, G_s, B_s) *using an example. The subscript "o" denotes original image, "d" denotes distorted image, "c" denotes compensated image, and "s" denotes compensated image displayed with a blue light blocker.*

This way, the compensated RGB value (R_c, G_c, B_c) is guaranteed to be within the display gamut. [1]

6 Experimental Results

In this section, we describe the experiments conducted to evaluate the proposed approach and show the results. Specifically, two experiments are conducted: One evaluates the blue light blocker described in Sec. 4, and the other evaluates the performance of the color compensation algorithm described in Sec. 5.

6.1 Optimized Blue Light Blocker

In this experiment, we optimize the spectral transmittance profile of the blue light blocker using the method described in Sec. 4. The emission spectra of the RGB primaries $r(\lambda)$, $g(\lambda)$, and $b(\lambda)$ of the ASUS PA246Q liquid crystal display (LCD) adopted in our experiment are measured with an PR-655 spectroradiometer, and the gamma values are estimated with a Laiko DT-101 colorimeter. The measured spectra of the RGB primaries are shown in Fig. 5.

Spectral transmittance Fig. 6 shows the spectral transmittance profile of the optimized blue light blocker. We can see that it is a notch filter and the stopband extends approximately from 450nm to 525 nm. Note that the stopband covers the most sensitive band of

[1] Patent pending.

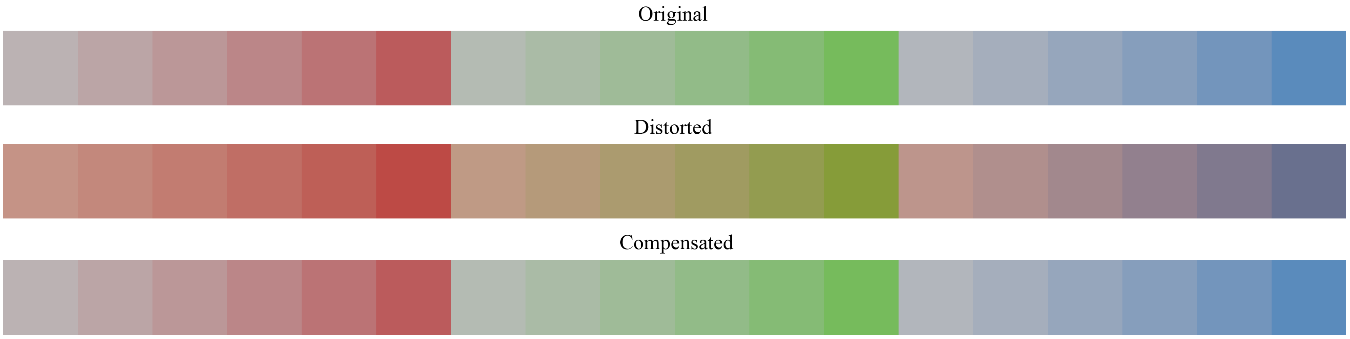

Figure. 9: *The original color patches* (*top*), *the distorted ones after applying the light blocker* (*middle*), *and the compensated results* (*bottom*).

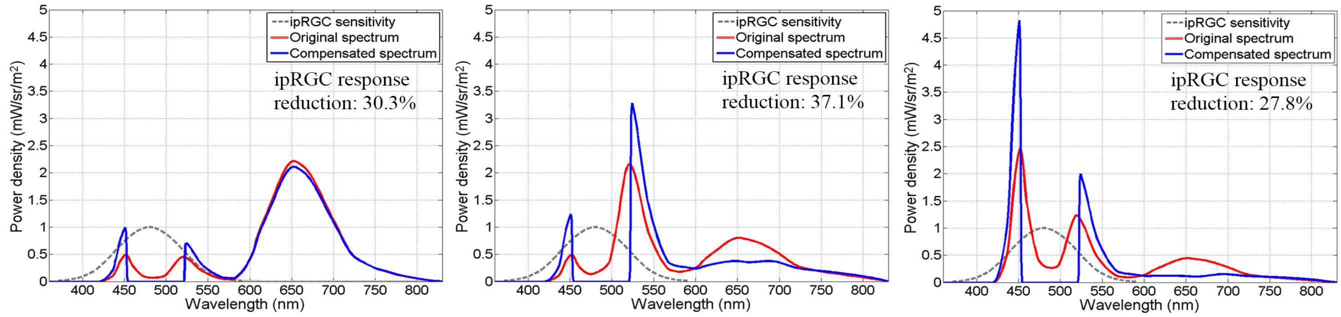

Figure. 10: *The original and compensated spectra of three sample colors. The original spectra are emitted from the display without any light blocker, and the compensated spectra are adjusted by our compensation algorithm and are emitted from the display with the optimized blue light blocker. The reduction percentage of ipRGC response is shown on the figure.*

the ipRGC centered at 482nm as expected. This blue light blocker reduces the expected value of the ipRGC response (8) by 62.6%.

Display gamut Fig. 7 shows the display gamut before and after applying the optimized blue light blocker. In the three-dimensional (3D) XYZ space shown in Fig. 7(a), the gamut volume after applying the blocker is 34.3% of the original gamut. However, contrary to the dramatic shrinkage of the 3D gamut, we can see in Figs. 7(b) that the area of each gamut in the two-dimensional (2D) xy space is approximately the same. In fact, the area of the gamut after the blocker is applied is even slightly larger (101.4%) than that of the original one. This result suggests that, although the light blocker reduces the maximum luminance of the display, it only slightly changes the range of chroma and hue.

6.2 Color Compensation

In this experiment, we compensate for the color distortion caused by the optimized blue light blocker described in Sec. 6.1 using the proposed compensation algorithm. This experiment consists of two parts. In the first part, uniform color patches are used as input. In the second part, natural images are used as input.

The results should be evaluated on an electronic display instead of a printout. Since the reader may not have a physical blue light blocker when evaluating the results, we simulate the appearance of the distorted image using the estimated display parameters. Specifically, the RGB value (R_d, G_d, B_d) of the distorted images and the RGB value (R_s, G_s, B_s) of the compensated images are generated by setting

$$\mathbf{H}\begin{bmatrix} R_d & G_d & B_d \end{bmatrix}^{\mathrm{T}} = \mathbf{H}_F\begin{bmatrix} R_o & G_o & B_o \end{bmatrix}^{\mathrm{T}} \tag{15}$$

and

$$\mathbf{H}\begin{bmatrix} R_s & G_s & B_s \end{bmatrix}^{\mathrm{T}} = \mathbf{H}_F\begin{bmatrix} R_c & G_c & B_c \end{bmatrix}^{\mathrm{T}}. \tag{16}$$

An illustration of the image notations used so far is given in Fig. 8.

Color patches In this part of the experiment, we apply our compensation algorithm to all 2^{24} colors in the 8-bit RGB space and compute their average color difference, chromatic difference, and the reduction rate of ipRGC response relative to the original image without blue light blocking. The CIE L*C*h* color difference ΔE^*_{ab} and the chromatic difference ΔC^*_{ab} are defined by

$$\Delta E^*_{ab} = \sqrt{\Delta L^2 + \Delta C^2 + \Delta h^2}, \tag{17}$$

$$\Delta C^*_{ab} = \sqrt{\Delta C^2 + \Delta h^2}, \tag{18}$$

where ΔL, ΔC, and Δh, respectively, represent the difference of lightness, chroma, and hue. Our experimental results show that the average ΔE^*_{ab} is 10.2, the average ΔC^*_{ab} is 2.8, and the average ipRGC reduction rate is 50.3%. In comparison, the average ΔE^*_{ab} and ΔC^*_{ab} without compensation are 31.1 and 29.4, respectively. Therefore, our compensation method reduces 67.2% of the CIE L*C*h* color difference and 90.5% of the chromatic difference. The average ΔE^*_{ab} is higher than the average ΔC^*_{ab} due to the fact that our compensation strategy attempts to compress the lightness of out-of-gamut pixels while preserving their hue and chroma.

For the reader to have a good feel of the performance of our color compensation method, we show eighteen sample colors in Fig. 9. It can be seen that the compensated colors are almost indistinguishable from the original ones. To illustrate the effect of our color compensation algorithm on the ipRGC response, we show in Fig. 10 the spectra of three sample colors (the 6th, 12th, and 18th color from the left in Fig. 9). We can see that the compensated spectra have extremely low power near the most sensitive band of ipRGC.

Natural images In this part of the experiment, we apply our color compensation algorithm to natural images. The compensated

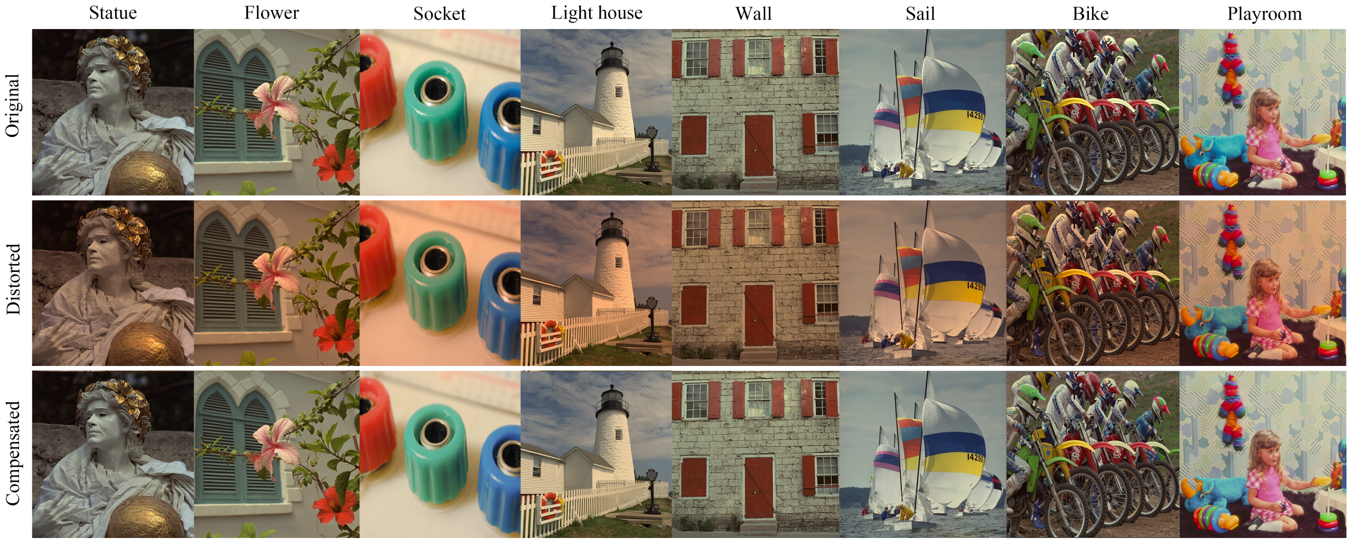

Figure. 11: *The compensated results for eight natural images. The first row shows the original images, the second row shows the distorted images, and the third row shows the compensated images.*

Figure. 12: *The ipRGC reduction percentage for the eight natural images shown in Fig. 11.*

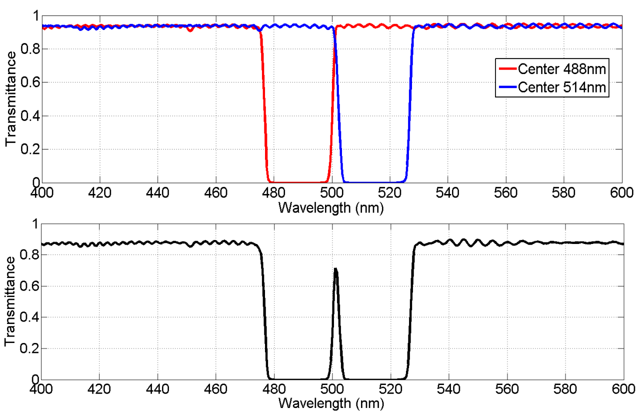

Figure. 13: (*a*) *The spectral transmittance profile of the two notch filters we adopt in the prototype.* (*b*) *The spectral transmittance profile of the light blocker constructed by concatenating the two notch filters.*

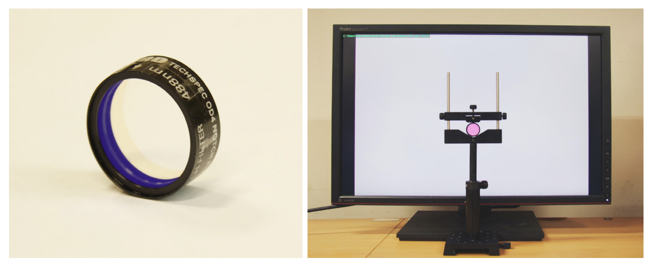

Figure. 14: (*Left*) *The light blocker consisting of two cascaded optical notch filters.* (*Right*) *The light blocker is mounted on a holder and placed in front of an LCD.*

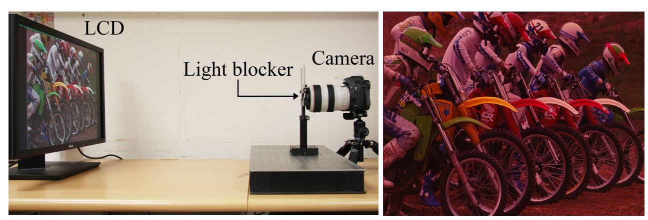

(a) (b)

Figure. 15: (*a*) *The setup of the experiment described in Sec. 7.2.* (*b*) *An example image captured with the light blocker.*

images and the ipRGC reduction rate, respectively, are shown in Figs. 11 and 12. We can see that dark and middle-toned colors (e.g. see the statue and the brick wall areas) are well preserved. In addition, for bright colors (e.g. the specular highlight on the sphere in the statue image, the white helmet and mudguard in the bike image, etc.) that cannot be perfectly preserved due to the limited display gamut, our method can still preserve the hue and chroma very well and make the compensated images appear similar to the original ones. Finally, it should be noted that the ipRGC response is reduced for all pixels whether they are within the gamut or not.

7 Prototype

A prototype display is implemented to validate our idea. In this section, we describe the prototype and evaluate its performance.

7.1 Optical Notch Filter

As pointed out in Sec. 6.2, an optical notch filter is needed in our prototype. A perfect notch filter that matches our specifications is difficult to find. Most off-the-shelf notch filters have a much narrower stopband. Therefore, in our prototype we cascade two notch filters with stopbands centered at 488nm and 514nm, as shown in Fig. 13(a). The spectral transmittance profile of the resulting light blocker is shown in Fig. 13(b). The experimental

Figure. 16: *The original, distorted, and compensated images displayed on our prototype. All images are captured with a digital camera.*

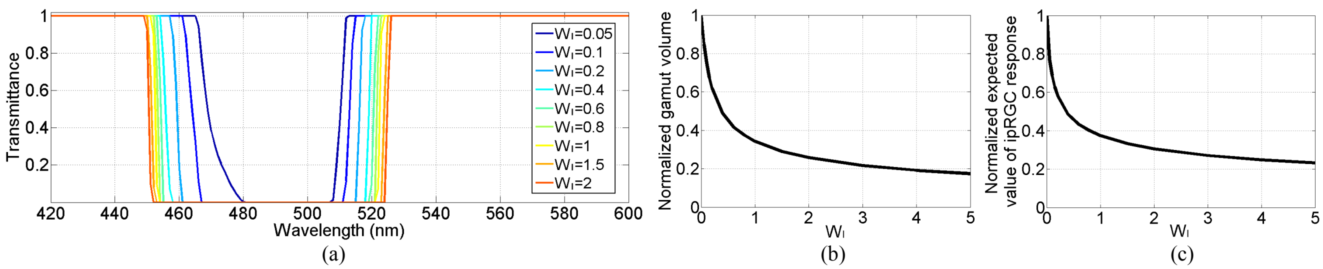

Figure. 17: (*a*) *The spectral transmittance profiles of the light blockers obtained by setting W_l to various values in* (*11*). (*b*) *The resulting normalized gamut volume as a function of W_l used to generate the light blocker.* (*c*) *The expected value of normalized ipRGC response as a function of the weight W_l.*

setup is shown in Fig. 14, where the light blocker is placed in front of an LCD and each notch filter is 25mm in diameter. To see the displayed image through the blocker, a user needs to hold the blocker near the eyes.

7.2 Evaluation

Effect of Non-optimized Filters The spectral transmittance profile of the light blocker used in the prototype is not exactly the same as that of the optimized light blocker. First, it does not completely block the light in the 450nm–476nm band. Second, it has a narrow passband centered at 501nm as a result of the gap between the stopbands of the two notch filters. Third, the transmittance in the passband is approximately 87% rather than 100%. In the following, we investigate the impact of these differences on the ipRGC reduction rate and color quality.

Similar to the experiment in Sec. 6.2, we examine the average ipRGC response reduction rate, CIE $L^*C^*h^*$ color difference ΔE^*_{ab}, and the chromatic difference ΔC^*_{ab} to evaluate the color quality of the prototype. The ipRGC response reduction rate is derived from the emission spectra measured by a spectroradiometer, while ΔE^*_{ab} and ΔC^*_{ab} are calculated using the XYZ values measured by a colorimeter. Experimental results show that the average ipRGC response reduction rate of the prototype is 42.9%. In comparison, the average ipRGC reduction rate of the optimized light blocker is 50.3% (see Sec. 6.2). The difference is 7.4%. On the other hand, the average ΔE^*_{ab} and ΔC^*_{ab} of the prototype are 9.6 and 3.0, respectively. For the optimized light blocker, ΔE^*_{ab} and ΔC^*_{ab} are 10.2 and 2.8, respectively. We can see that although the prototype has a slightly larger chromatic difference, it has a lower color difference. The lower color difference is due to the existence of the 450nm–476nm passband, which allows a slight amount of additional blue light to pass through.

Image quality To demonstrate the image quality of the prototype, we capture images displayed on the prototype by a Canon EOS 7D Mk. II digital camera. In the capturing process, we place the light blocker right in front of the camera, as shown in Fig. 15(a). Without color compensation, the displayed image suffers severe color distortion, as illustrated in Fig. 15(b).

Because the spectral sensitivity of the camera is different from the XYZ color matching functions of the human visual system, we first calibrate the display-camera system using the technique developed

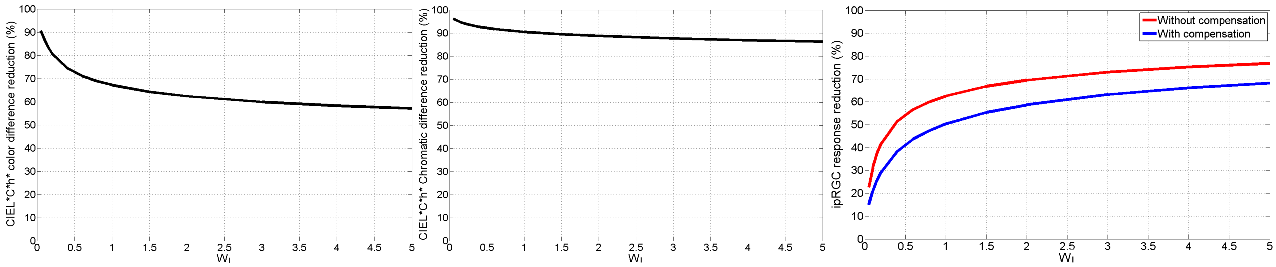

(a) (b) (c)

Figure. 18: (*a*) *The average reduction percentage of CIE L*C*h* distance as a function of W_I.* (*b*) *The average reduction percentage of chromatic distortion as a function of W_I.* (*c*) *The average ipRGC reduction percentage as a function of W_I with and without color compensation.*

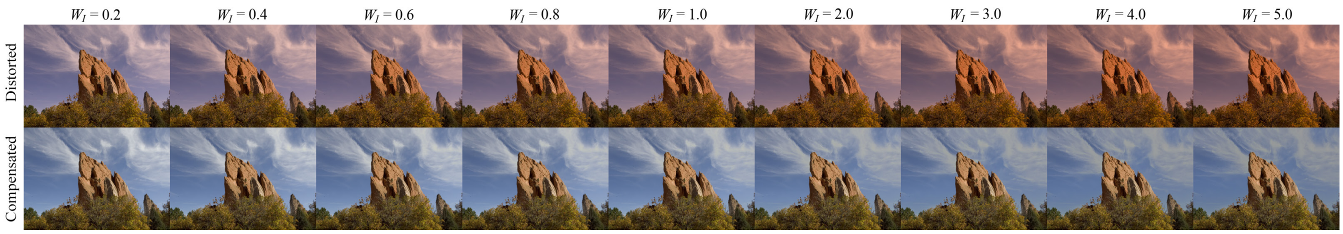

Figure. 19: *The distorted images in the top row demonstrate the color distortion caused by blue light blockers with different stopband widths, and the compensated images in the bottom row demonstrate the compensation quality of our algorithm.*

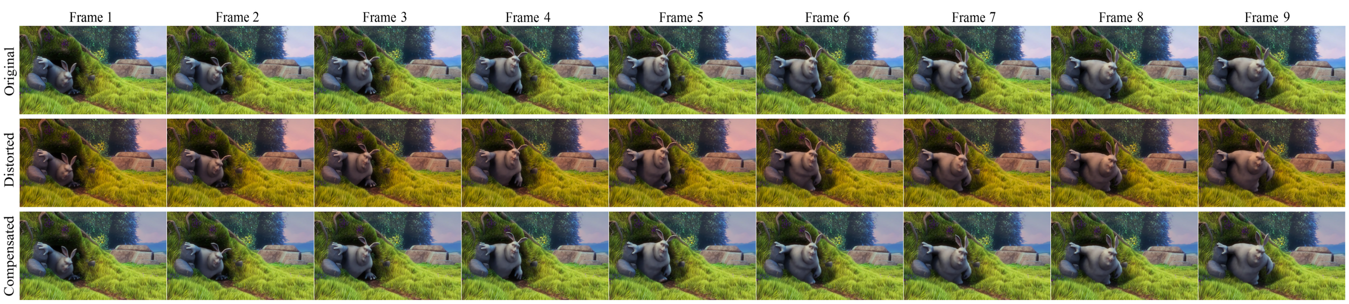

Figure. 20: *Nine consecutive frames of the original video, the distorted video, and the compensated video.*

for projector-camera systems [Liu et al. 2015] and then perform color compensation by substituting the matrices $\mathbf{H}_F$ and $\mathbf{H}$, respectively, with the color mixing matrix obtained with and without the light blocker.

During the capturing process, the auto white balance function is turned off, and all camera parameters (exposure time, aperture size, ISO, white point, etc.) remain fixed. The compensated results for 45 test images are shown in Fig. 16. We can see that, although the compensated images are slightly dimmer than the original images for some regions, they do have similar color appearance as expected.

8 Discussion

In this section, we discuss the effect of the stopband width of the light blocker, the lightness reduction caused by color compensation, the speed of the compensation algorithm, application to dynamic contents, the cost, and the limitations of this work.

8.1 Stopband Width

To investigate the effect of stopband width on color fidelity and ipRGC response, we generate a series of spectral transmittance profiles by varying the weight w_I in Algorithm 1 and examine the performance of our color compensation method for these spectral transmittance profiles.

The generated spectral transmittance profiles are plotted in Fig. 17(a). We can see that the stopband becomes wider as w_I increases. We also show the gamut volume and the expected ipRGC response, respectively, in Fig. 17(b) and (c) as functions of w_I. We can see that, as w_I increases, the display gamut shrinks and the expected ipRGC response decreases.

To evaluate color fidelity, we again examine the average ΔE^*_{ab} and ΔC^*_{ab} for colors in the RGB space. Specifically, we compare ΔE^*_{ab} and ΔC^*_{ab} of the distorted colors with those of the compensated colors and calculate the reduction rate. The results are shown in Fig. 18. We can see that our compensation algorithm reduces the ΔE^*_{ab} by more than 58% and ΔC^*_{ab} by more than 87%. From the ipRGC response reduction rate shown in Fig. 18(c), we can see that the ipRGC response reduction rate only drops by approximately 10%. Overall, our compensation algorithm can reduce color distortion effectively at the expense of a slight increase of the ipRGC response.

From the compensated images shown in Fig. 19, we can see that, despite the increase of stopband width of the light blocker, our compensation algorithm is capable of restoring the image appearance.

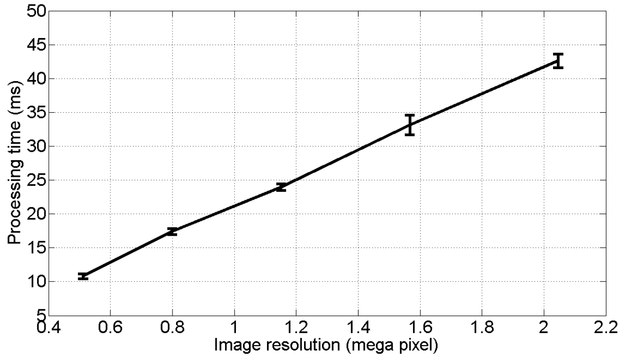

Figure. 21: *The computation time of our color compensation algorithm.*

8.2 Dynamic Content

In addition to still images, our color compensation algorithm can be applied to videos by processing each frame independently. The compensated video generated this way does not have flickering artifact, and no additional temporal smoothing is required. Fig. 20 shows nine consecutive frames of the original video, the distorted video, and the compensated video. We can see that the color of the processed frames is consistent along the time axis.

8.3 Computation Time

To test the speed of our color compensation algorithm, we apply it to images of various resolutions and record the execution time. Our algorithm is implemented in Matlab on a desktop computer running Windows 7 and with a 3.60 GHz Intel Core i3-4160 and a 6GB memory. The results are shown in Fig. 21. We can see that the program is able to process more than 20 frames per second for an image having more than 2 mega pixels. The execution time of our pure software implementation here only serves as a reference. The computation can be further accelerated by hardware if needed.

8.4 Cost

The notch filters adopted in our prototype are expansive because they have very narrow stopband and sharp transition edge between the stopband and the passband. There are two possible ways to reduce the cost. First, the specification of the notch filter may be compromised. For example, the transition edge may be made smoother and the stopband may be made wider. How to strike a balance between cost and performance degradation caused by such compromise is a topic for future research. Second, the filter can be placed on the eyewear instead of the display to reduce the filter size and, consequently, the cost. Our technique is also suitable for near-eye displays such as those on virtual-reality devices, for which the filter size is limited.

8.5 Limitations

We discuss two limitations of this work. First, we cannot preserve the exact appearance of bright colors due to limited dynamic range of the display. Second, our color compensation method may be less effective for displays with narrow-band primaries. Specifically, if the spectral power of the blue primary is highly concentrated near the sensitive band of ipRGC, poor color compensation quality is expected because almost all the emission power of the blue primary is blocked. Fortunately, as shown in Fig. 3, most existing displays adopt a wide-band light source.

8.6 Psychophysical Test

This work is built upon the findings in psychology and medical science about the ipRGC response. In this paper, we show the emission spectrum of a display and the effectiveness of color compensation to support our claim. However, we are unable to conduct a psychophysical test on human health. It is a long-term, delicate experiment that may take years to complete and requires expertise beyond our technical skills. Given the correlation between ipRGC response and melatonin suppression found in previous studies, we feel that the quantitative evaluation described in Sec. 6.2 and Sec. 7.2 are sufficient to justify our method from the engineering perspective.

9 Conclusion

In this paper, we have shown that it is possible to reduce harmful blue light for a display panel without degrading image color appearance. Based on the psychophysical characteristics of ipRGC, we have derived the spectral transmittance profile of the blue light blocker that maximizes the display gamut and minimizes the ipRGC response. In addition, we have described an algorithm to compensate for the color distortion caused by a blue light blocker. We have also built a proof-of-concept prototype to demonstrate the feasibility of our approach.

References

BERSON, D. M., DUNN, F. A., AND TAKAO M. 2002. Phototransduction by retinal ganglion cells that set the circadian clock. *Science*, vol. 295, 5557, 1070–1073.

BERSON, D. M. 2003. Strange vision: ganglion cells as circadian photoreceptors. *Trends in Neurosciences*, vol. 26, 6, 314–320.

CHANG, A. M., AESCHBACH, D., DUFFY, J. F., AND CZEISLER, C. A. 2015. Evening use of light-emitting eReaders negatively affects sleep, circadian timing, and next-morning alertness. In *Proceedings of the National Academy of Sciences*, 112, 4, 1232–1237.

DACEY, D. M., LIAO H. W., PETERSON, B. B., ROBINSON, F. R., SMITH, V. C., POKORNY, J., YAU, K.-W., AND GAMLIN., P. D. 2005. Melanopsin-expressing ganglion cells in primate retina signal colour and irradiance and project to the LGN. *Nature* 433, 749–754.

FAIRCHILD, M. D. 2005. *Color Appearance Models*, 2nd ed. Wiley-IS&T, Chichester, UK.

GALINDO-ROMEROA, C., JIMÉNEZ-LÓPEZA, M., GARCÍA-AYUSOA, D., SALINAS-NAVARROA, M., NADAL-NICOLÁSA, F.M., AGUDO-BARRIUSOA, M., VILLEGAS-PÉREZA, M.P., AVILÉS-TRIGUEROSA, M., AND VIDAL-SANZA, M. 2013. Number and spatial distribution of intrinsically photosensitive retinal ganglion cells in the adult albino rat. *Experimental Eye Research*, vol. 108, 84–93.

GAMLIN, P. D. R., MCDOUGAL, D. H., POKORNY, J, SMITH, V. C., YAU, K.-W., AND DACEY, D. M. 2007. Human and macaque pupil responses driven by melanopsin-containing retinal ganglion cells. *Vision Research*, vol. 47, 7, 946–954.

HARVARD HEALTH LETTER, 2012. Blue light has a dark side. http://www.health.harvard.edu/staying-healthy/blue-light-has-a-dark-side.

LELY, S., FREY, S., GARBAZZA, C., WIRZ-JUSTICE, A., JENNI, O.G., STEINER, R., WOLF, S., CAJOCHEN, C., BROMUNDT, V., AND SCHMIDT, C. 2014. Blue blocker glasses as a countermeasure for alerting effects of evening light-emitting diode screen exposure in male teenagers. *Journal of Adolescent Health*, vol. 56, 1, 113–119.

LINDBLOOM, B. J. 1989. Accurate color reproduction for computer graphics applications. *ACM Computer Graphics*, vol. 23, 3, 117–126.

LIU, J.-S., SHIH, K.-T., AND CHEN, H. H. 2015. Preserving image color appearance on non-white projection surfaces. In *Proceedings of IEEE Int. Conf. Multimedia & Expo*, 1–6.

MIYAZAKI, D., NAKAMURA, K., BABA, M, FURUKAWA R., AOYAMA, M., HIURA, S., AND ASADA, N. 2012. A first introduction to metamerism art. *SIGGRAPH Asia Posters*, 17.

MOROVIC, J. 2008. *Color gamut mapping*. John Wiley & Sons.

REINHARD, E., POULI, T., KUNKEL, T., LONG, B., BALLESTAD, A., AND DAMBERG, A. 2012. Calibrared Image Appearance Reproduction. *ACM Transactions on Graphics*, vol. 31, 6, 201.

ROECKLEIN, K. A., ROHAN, K. J., DUNCAN, W. C., ROLLAG, M. D., ROSENTHAL, N. E., LIPSKY, R. H., AND PROVENCIO, I. 2009. A missense variant (P10L) of the melanopsin (Opn4) gene is associated with seasonal affective disorder. *Journal of Affective Disorders*, vol. 114, 1–3, 279–285.

SHAPIRA, L. AND OICHERMAN, B. 2012. Black is green: adaptive color transformation for reduced ink usage. *Comput. Graph. Forum*, vol.31, 2, 365–372.

SHIH, K.-T. AND CHEN, H. H. 2016. Exploiting perceptual anchoring for color image enhancement. *IEEE Transactions on Multimedia*, vol.18, 2, 300–310.

SHIH, K.-T., CHEN, H. H., AND LIU, Y.-N. 2016. Image processing system and method. Publication No. US20160093268 A1. Filed Sept. 30, 2014.

SMITH, T. AND GUILD, J. 1931. The C.I.E. colorimetric standards and their use. *Trans. Optical Soc.*, vol. 33, 3, 73–134.

STEVENS, R. G., BLASK, D. E., BRAINARD, G. C., HANSEN, J., LOCKLEY, S. W., PROVENCIO, I., REA, M. S. AND REINLIB, L. 2007. Meeting report: The role of environmental lighting and circadian disruption in cancer and other diseases. *Environmental Health Perspectives*, vol. 115, 9, 1357–1362.

STEVENS, R. G. 2009. Light-at-night, circadian disruption and breast cancer: assessment of existing evidence. *International Journal of Epidemiology*, vol. 38, 4, 963–970.

WANAT, R. AND MANTUIK, R. K. 2014. Simulating and compensating changes in appearance between day and night vision. *ACM Transactions on Graphics*, vol. 33, 4, 1–12.

WONG, K. Y. 2012. A retinal ganglion cell that can signal irradiance continuously for 10 hours. *Journal of Neuroscience*, vol. 32(33), 11478–11485.

ZAIDI, F. H., HULL, J. T., PEIRSON, S. N., WULFF, K., AESCHBACH, D., GOOLEY, J. J., BRAINARD, G. C., GREGORY-EVANS, K., RIZZO III, J. F., CZEISLER, C. A., FOSTER, R. G., MOSELEY, M. J., AND LOCKLEY, S. W. 2007. Short-wavelength light sensitivity of circadian, pupillary, and visual awareness in humans lacking an outer retina. *Current Biology*, vol. 17, 24, 2122–2128.